ME404 Fluid flow

Buildings and their energy supply systems (conventional and renewable) can be thought of as comprising three interacting fluid flow domains as summarised in figure 1:

1. air/vapour flow through cracks and openings in the building envelope allowing infiltration and natural ventilation;
2. the flow of air/vapour through the leakage paths connecting internal spaces and the distribution networks that exist to service the building's heating, cooling and ventilation demands; and
3. the movement of air/vapour/pollutants within the interior spaces of the building or the movement of working fluids within plant components.

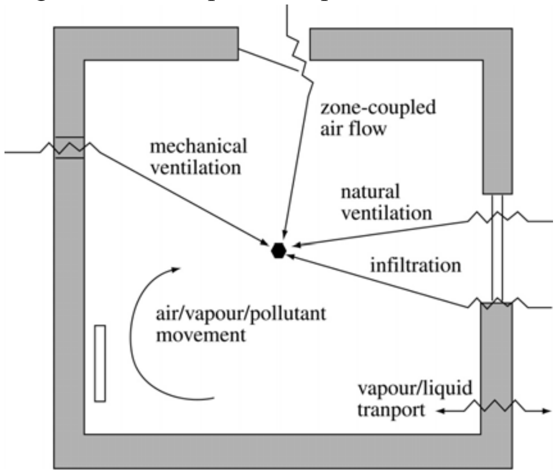

Figure 1: Building fluid flow domains.

There are essentially two modelling approaches suitable for application to these domains: nodal networks (applicable to domains 1 and 2) and computational fluid dynamics (applicable to domain 3).

1. Nodal network method

The building and its air handling systems are treated as a collection of nodes representing rooms (or parts of rooms), equipment connection points, ambient conditions etc. Inter-nodal connections are then defined in terms of components such as cracks, doors, fans, ducts etc, each represented by a model that gives the mass flow rate as a function of the pressure difference across the component. Consideration of the conservation of mass at each node leads to a set of non-linear equations that can be solved at successive time steps to characterise the flow throughout the defined network.

The method is constrained to the steady flow of an incompressible fluid within a network of connected pressure points (nodes) when subjected to successive sets of boundary conditions. In other words, the problem reduces to the calculation of the mass flows through each connection when the nodes represent internal (unknown) and external (known) pressures. Solution for a particular boundary condition is achieved by an iterative approach in which the unknown nodal pressures are repeatedly adjusted until the nodal mass imbalances (residuals) are reduced to insignificance. The flow network may comprise sub-networks, each relating to a different fluid type.

Boundary conditions

In the case of buildings, the surface pressure distribution is wind induced. Its prediction requires information on the prevailing wind\(emits speed, direction and vertical velocity profile – and, more problematic, the influence of local obstructions and terrain features. Two approaches to the determination of surface pressure distribution are extant: wind tunnel tests applied to scale models, and the use of mathematical models. Whatever the approach, it is usual to express the outcome for a given surface in the form of a dimensionless pressure coefficient set as shown in figure 2.

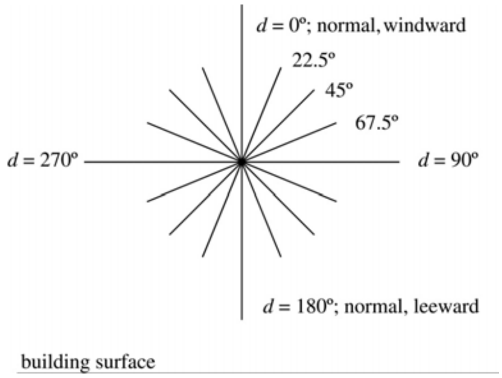

Figure 2: A surface pressure coefficient set.

For any given wind direction, d:

$$C_{id} = \frac{P_{id}}{\frac{1}{2}\rho v_r^2}$$

where C_{id} is the pressure coefficient for surface i and corresponding to a wind direction d, P_{id} the surface pressure (N/m^2), ρ the air density (kg/m^3) and v_r some reference wind speed corresponding to direction d (m/s).

A pressure coefficient set typically comprises 16 compass values at 22.5° intervals so that the coefficient for any particular wind direction may include the influence of an obstruction feature. Note that coefficients can be negative to reflect leeward exposures. Table 1 gives some example pressure coefficient sets for some typical exposures and building length-to-width ratios.

Table 1: Pressure coefficient sets.

Pressure coefficients at 22.5° intervals	Context
0.70/0.53/0.35/-0.08/-0.50/-0.45/-0.40/-0.30/-0.20/-0.30/-0.40/-0.45/-0.50/-0.08/0.35/0.53	1:1 exposed wall
0.20/0.13/0.05/-0.10/-0.25/-0.23/-0.30/-0.28/-0.25/-0.28/-0.30/-0.28/-0.25/-0.10/0.05/0.13	1:1 sheltered wall
0.50/0.38/0.25/-0.13/-0.50/-0.65/-0.80/-0.75/-0.70/-0.75/-0.80/-0.65/-0.50/-0.13/0.25/0.38	2:1 exposed long wall
0.06/-0.03/-0.12/-0.16/-0.20/-0.29/-0.38/-0.34/-0.30/-0.34/-0.38/-0.29/-0.20/-0.16/-0.12/-0.03	2:1 sheltered long wall
0.60/0.40/0.20/-0.35/-0.90/-0.75/-0.60/-0.48/-0.35/-0.48/-0.60/-0.75/-0.90/-0.35/0.20/0.40	1:2 exposed short wall
0.18/0.17/0.15/-0.08/-0.30/-0.31/-0.32/-0.26/-0.20/-0.26/-0.32/-0.31/-0.30/-0.08/0.15/0.16	2:1 sheltered short wall
-0.80/-0.75/-0.70/-0.65/-0.60/-0.55/-0.50/-0.45/-0.40/-0.45/-0.50/-0.55/-0.60/-0.65/-0.70/-0.75	1:1 exposed roof <10°
-0.40/-0.45/-0.50/-0.55/-0.60/-0.55/-0.50/-0.45/-0.40/-0.45/-0.50/-0.55/-0.60/-0.55/-0.50/-0.45	1:1 exposed roof 10-30°
0.30/-0.05/-0.40/-0.50/-0.60/-0.50/-0.40/-0.45/-0.50/-0.45/-0.40/-0.50/-0.60/-0.50/-0.40/-0.05	1:1 exposed roof >30°
-0.70/-0.70/-0.70/-0.75/-0.80/-0.75/-0.70/-0.70/-0.70/-0.70/-0.70/-0.75/-0.80/-0.75/-0.70/-0.70	2:1 exposed roof <10°
-0.70/-0.70/-0.70/-0.70/-0.70/-0.65/-0.60/-0.55/-0.50/-0.55/-0.60/-0.65/-0.70/-0.70/-0.70/-0.70	2:1 exposed roof 10-30°
0.25/0.13/0.00/-0.30/-0.60/-0.75/-0.90/-0.85/-0.80/-0.85/-0.90/-0.75/-0.60/-0.30/0.00/0.13	2:1 exposed roof >30°

Where the reference wind speed, v_r, is a local wind speed, it is necessary to modify the free stream wind speed as a function of any height difference and the effect of local terrain roughness. This requires the use of an assumed wind profile.

Node definition

It is assumed that nodes (representing discrete, homogeneous fluid volumes) can be characterised by a single temperature, a single static pressure and a height relative to some arbitrary datum. Table 2 lists some possible node types and their typical defining data.

Table 2: Node types and defining parameters.

Internal, unknown condition	height
Internal, known condition	height, total pressure and temperature
Boundary, known pressure	height, total pressure and temperature
Boundary, wind pressure	height, pressure coefficient set, surface azimuth

Of course, internal node temperatures are not required where the flow network is to be combined with a building/plant equation-set.

Buoyancy effects

Consider figure 3, which shows two zones connected by a duct. The zone height is typically given as the average height of all openings when expressed relative to some convenient datum. For the case shown, the ends of the duct are at different heights relative to each other and relative to the nodes representing the zones.

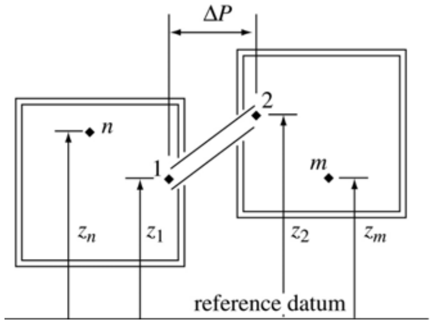

Figure 3: Two connected zones.

The pressure drop across the component may be determined from Bernoulli's equation for the one-dimensional steady flow of an incompressible fluid:

$$\Delta P = \left(p_1 + \rho V_1^2/2\right) - \left(p_2 + \rho V_2^2/2\right) + \rho_i g\left(z_1 - z_2\right); i = n, m \qquad \ldots (1)$$

where ΔP is the sum of all friction and dynamic losses (N/m^2), p_1, p_2 the entry and exit static pressures (Pa), V_1, V_2 the entry and exit velocities (m/s), ρ the density of the air flowing through the component (kg/m^3; i=n or m depending on the direction of the flow), g the acceleration of gravity (m/s^2 and z_1, z_2 the entry and exit elevations (m). This equation defines a sign convention for the flow direction: positive from point 1 to point 2 (n to m).

In the above equation dynamic pressures are the $\rho V^2/2$ terms, and total pressure is defined to be the sum of static pressure and dynamic pressure, i.e. $P = p + \rho V^2/2$. If nodes n and m represent large volumes, the dynamic pressures are effectively zero. If the nodes represent some point in a duct or pipe network, there will be a positive dynamic pressure. The pressures at the inlet and outlet of the flow component can be related to the node pressures by the hydrostatic law:

$$P_1 = P_n + \rho_n g(z_n - z_1) = P_n - \rho_n g h_1$$

where $h_1 = z_1 - z_n$, and

$$P_2 = P_m + \rho_m g(z_m - z_2) = P_m - \rho_m g h_2$$

where $h_2 = z_2 - z_m$.

Ignoring dynamic pressures, equation (1) reduces to

$$\Delta P = P_n - P_m + \rho_i g(z_n + h_1 - z_m - h_2) - \rho_n g h_1 + \rho_m g h_2; i = n, m.$$

The terms $\rho g(z_n + h_1 - z_m - h_2)$, $-\rho_n g h_1$ and $\rho_m g h_2$ are collectively termed the stack pressure, PS, acting on the component:

$$PS = \rho_n g(z_n - z_m) + h_2 g(\rho_m - \rho_n) \quad \text{; for the +ve direction}$$

$$PS = \rho_n g(z_n - z_m) + h_2 g(\rho_m - \rho_n) \quad \text{; for the –ve direction.}$$

Component flow models

A flow component is characterised by a type (duct, pipe, pump, crack, doorway etc.) and a number of defining parameters. Table 3 list some typical component types and models.

Table 3: Flow component types and models.

Component	Model
Power law volume flow resistance	$m = \rho\ a\ \Delta P^n$
Power law mass flow resistance	$m = a\ \Delta P^b$
Power law mass flow resistance	$m = a\sqrt{(\rho.\Delta P^b)}$
Quadratic law volume flow resistance	$\Delta P = a\ m/\rho + b(m/\rho)^2$
Quadratic law mass flow resistance	$\Delta P = a\ m + b\ m^2$
Constant volume flow rate component	$m = \rho\ r_v$
Constant mass flow rate component	$m = r_m$
Common orifice flow component	$m = C_d A\sqrt{(2\rho\Delta P)}$
Laminar pipe flow component	$m = \rho\Delta P\ \pi\ R^4/8\mu\ L_p$
Specific air flow opening	$m = 0.65A\sqrt{(2\rho\Delta P)}$
Specific air flow crack	$m = f(\rho, k, \Delta P)$
Specific air flow door	$m = f(W_d, H, H_r, C_d, \Delta P)$
General flow conduit (duct or pipe)	$m = A_c \sqrt{((2\rho\Delta P)/(f\ L_p/D_h + \Sigma C_i))}$; $f=1/2\log(5.74/Re^{0.901}+0.27\ k_r/D_h)^2$
General flow inducer (pump or fan)	$\Delta P = \Sigma^3_{i=0}\ a_i(m/\rho)^i$; $q_{mn} \le m/\rho \le q_{mx}$
General flow corrector	$m = \rho k_v(\Delta P\rho_0/\Delta P_0\rho)$
Flow corrector with polynomial local loss	$m = A_c[(2\rho\Delta P)/C]^{1/2}$; $C = \Sigma^3_{i=0}a_i(H/H_{100})^i$
Ideal (frictionless) open/shut flow controller	$m = 0$ or $m = \rho q$

where m is the mass flow rate (kg/s, a and b are empirical coefficients, n is an empirical exponent, r_v the volume flow rate (m^3/s), r_m the mass flow rate (kg/s), A the opening area (m^2), C_d the discharge factor (-), μ the dynamic viscosity (kg/m.s), Re the Reynolds Number, L_p the pipe length, R the pipe radius, W_c the crack width, L_c the crack length, W_d the door width, H the door height and H_r the door reference height; D_h is the hydraulic diameter, A_c the cross sectional area (m^2), k_r the pipe wall roughness (-),ΣC_i the sum of the local dynamic loss factors (-), q_{mn} & q_{mx} the minimum and maximum volume flow rates respectively (m^3/s), ρ & ρ_0 the density and standard density respectively (kg/m^3), ΔP_0 the standard pressure (N/m^2), k_v the volume flow rate at ρ_0 (m^3/s) and H & H_{100} are the valve position and fully open position respectively; (all linear dimensions in m).

Each component has a corresponding model for the evaluation of the flow rate as a function of the pressure drop. For example, a valve may be represented as a conduit with an empirically derived dynamic loss factor, C (-), which is dependent on the valve stem displacement. The mass flow rate, m, may then be calculated from

$$m = A(2\rho\Delta P/C)^{1/2}$$

$$C = a_0 + a_1 H/H_{100} + a_2(H/H_{100})^2 + a_3(H/H_{100})^3$$

where A is the cross-sectional area containing the corrector (m^2), H/H_{100} is the relative valve position (-), and a_i are fit coefficients (-).

In general, the equations that represent the air mass flow rate through simple restrictions may be expressed by an equation of the form

$$m = k.a\Delta P^x$$

where ΔP is the pressure difference across the restriction (N/m^2), k an empirical constant that depends on the nature of the flow restriction, 'a' a characteristic dimension such as length or area, and x an empirical exponent.

For a simple orifice at high Reynolds Number (such as a partially open window), x is close to 0.5. For cracks and similar restrictions with a large aspect ratio, x is close to 0.65, rising to unity for completely laminar flow. For this class of flow restriction empirical relationships have been established to determine x and k as a function of crack width:

$$x = 0.5 + 0.5\exp(-W/2)$$
$$k = 9.7(0.0092)^x$$

where W is the crack width (mm) and therefore 'a' becomes the crack length.

With open windows the flow rate (m^3/s) may be determined from

$$q = C_d A\sqrt{2\Delta P/\rho_i}$$

where C_d is the discharge coefficient (-), A the opening area (m^2), ΔP the pressure difference across the opening (Pa) and ρ_i the density of the incoming air (kg/m^3).

With large vertical openings, such as doorways, more complex flow patterns occur. If a temperature difference exists across such an opening, then air flow can occur in both directions due to the action of small density variations over the door height causing a positive pressure difference at the bottom (or top) of the opening with a corresponding negative pressure difference at the top (or bottom). This situation is illustrated in figure 4. A typical expression for the air flow through such an opening might appear as follows.

$$v = (2/3)[C_D Wh(2/\rho)^{1/2}(C_a^{1/2} - C_b^{1/2})/C_t]$$

where C_D is the discharge coefficient (-), W the opening width (m), h the height (m), $C_a = (1 - r_p)C_t + (P_1 - P_2)$, $C_b = (P_1 - P_2) - r_pC_t$, $C_t = gP_ah/R(1/\theta_2 - 1/\theta_1)$, θ_1, θ_2 the absolute temperatures on either side of the opening (K), P_a the atmospheric pressure (N/m^2), P_1, P_2 the pressures on either side (N/m^2), R the gas constant (J/kgK), $r_p = h_p/h$ and h_p is the height of the reference nodes on either side (m). On evaluation, this equation yields a sum of real and imaginary parts. Real parts indicate a flow in the positive direction, while imaginary parts indicate a flow in the reverse direction.

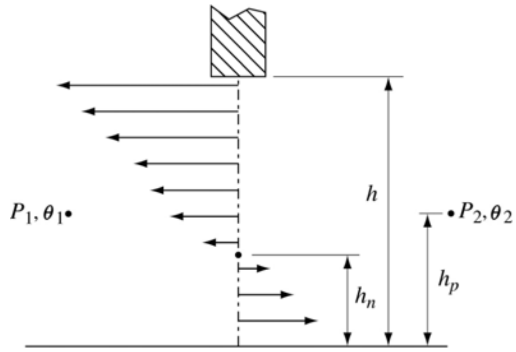

Figure 4: Bi-directional air flow across a doorway.

The neutral height h_n – the height at which no net pressure difference can be measured across an opening – is found from

$$h_n = h(r_p - (P_1 - P_2)/C_t) .$$

Iterative solution procedure

Each non-boundary node is assigned an arbitrary pressure and the connecting components' flow rates determined from the corresponding mass flow model as described in the previous section. The nodal mass flow rate residual (error), R_i (kg/s), for the current iteration is then determined from

$$R_i = \sum_{k=1}^{K_i} m_k$$

where m_k is the mass flow rate along the kth connection to node i and K_i is the total number of connections linked to node i.

These residuals are used to determine nodal pressures corrections, $\mathbf{P}^*$, for application to the current pressure field, $\mathbf{P}$:

$$\mathbf{P}^* = \mathbf{P} - \mathbf{C}$$

where $\mathbf{C}$ is a pressure correction vector. The process, which is equivalent to a Newton-Raphson technique, iterates until convergence is achieved. In the method $\mathbf{C}$ is determined from

$$\mathbf{C} = \mathbf{J}^{-1}\,\mathbf{R}$$

where $\mathbf{R}$ is the vector of nodal mass flow residuals and $\mathbf{J}^{-1}$ is the inverse of the square Jacobian matrix whose diagonal elements are given by

$$J_{n,n} = \sum_{i=1}^{L} \left(\frac{\partial \dot{m}}{\partial \Delta P} \right)_i$$

where L is the total number of connections linked to node n. This is equivalent to the rate of change of the node n residual with respect to the node pressure change between each iteration. The off-diagonal elements of $\mathbf{J}$ are the rate of change of the individual component flows with respect to the change in the pressure difference across the component (at successive iterations):

$$J_{n,m} = \sum_{i=1}^{M} -\left(\frac{\partial \dot{m}}{\partial \Delta P}\right)_i ; n \neq m$$

where M is the number of connections between node n and node m. Note that for internal nodes the summation of the elements comprising each row of the Jacobian matrix are identically zero.

Conservation considerations applied to each node then provide the convergence criterion at all internal nodes:

$$\sum m_k \to 0$$

In practice, the foregoing solution technique may be expected to solve even complex networks in a few iterations. This means that, unlike CFD, the network air flow method will not impose a significant computational burden. This renders the method most suitable for the modelling of combined thermal and flow problems.

The above approach can also be applied to form an electrical power flow model in which an electrical circuit is conceived as a network of nodes representing the junctions between conducting elements and locations where power is extracted to feed loads or added from the public electricity supply or local renewable energy systems. The solution of such a power flow network requires models for the connecting components (e.g. conductors), sources of power (e.g. photovoltaic components and wind turbines) and loads.

2. Computational fluid dynamics

This method is based on the solution of the conservation equations for mass, momentum and energy at discrete points within a room or plant component. For a given boundary condition, numerical methods are employed to solve for the temperature, pressure and velocity fields. It is also possible to determine the distribution of water vapour or pollutants, and to assess the mean age (freshness) of air at different locations within a room. Such information is the prerequisite of an appraisal of indoor air quality and discomfort.

Although well adapted for building energy application, the nodal network method is limited when it comes to consideration of indoor comfort and air quality. Because momentum effects are neglected, intra-room air movement cannot be studied, while surface convection heat transfer regimes cannot be evaluated because of the low resolution. To overcome these limitations, it is necessary to introduce a computational fluid dynamics (CFD) model whereby intra-zone air movement may be evaluated and the distribution of the principal parameters determined.

CFD is a complex development field with a rapidly evolving state-of-the-art and general applicability. In recent years its application to buildings – a non-steady, mixed flow (turbulent, laminar and transitional) problem – has grown significantly and attempts have been made to combine CFD and building energy models, to extend CFD to include building features and to develop techniques for the realistic representation of HVAC components such as diffusers.

Essentially, a building-integrated CFD model comprises the following elements: room discretisation; a set of equations to represent the conservation of energy, mass, momentum and species; the imposition of boundary conditions; an equation solver; and a method to link the CFD, building thermal and network air flow models.

Domain discretisation

The starting point is to sub-divide the room into a number of finite volumes so that conservation equations for mass, momentum, energy and species concentration may be established and solved for the entire domain. While curvilinear co-ordinate systems are commonly employed in CFD analyses, in building applications the geometries are typically orthogonal, facilitating the three dimensional Cartesian grid technique as illustrated in figure 5 in which each dimension is divided into a number of regions – here 3 in the x-direction and 2 in the z-direction; the y-direction is not shown. The regions are then gridded using a constant or variable spacing.

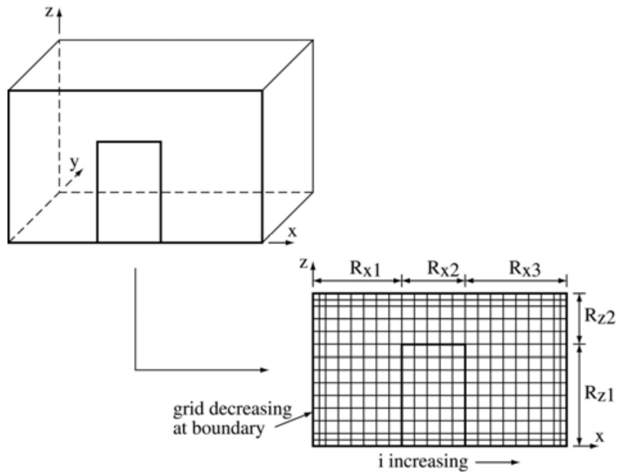

Figure 5: CFD domain discretisation.

Consider the x-direction: the region located to the left of the door has a variable grid which increases with increasing i, the door region has a constant grid, while the region located to the right of the door decreases with increasing i. Other approaches are possible, and some of these are suited to the case of low Reynolds Number models where the near-wall grid is made especially fine.

For the case of non-rectangular geometries, or where internal obstructions are present, the above technique may be applied to a rectangular bounding box but with the boundary of the non-participating cells treated as solid surfaces and assigned a boundary condition as shown in figure 6 (lower left).

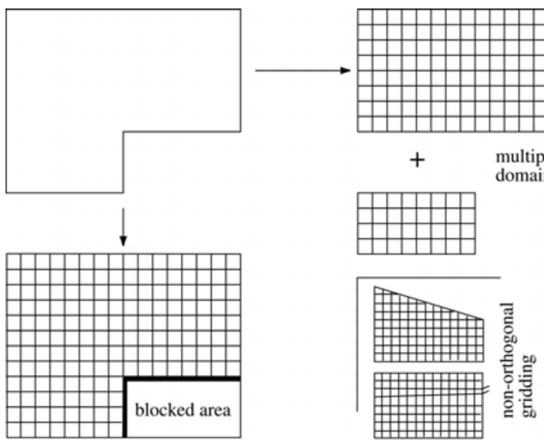

Figure 6: Treatment of complex geometries.

Alternatively, a block structured approach may be employed (figure 6, upper right) whereby the problem is reduced to separate domains which are then processed independently with the mass, momentum, energy and species exchanges at the interfaces reconciled after each iteration. Such a treatment facilitates the parallel processing of domains but will result in a large number of domains for cases where internal objects are included.

To accommodate the range of commonly encountered room shapes, the gridding scheme may be extended to allow one or more of the three dimensions to be non-orthogonal (figure 6, lower right).

Conserving energy, mass, momentum and species concentration

The movement of room air and contaminants may be determined from the solution of discretised mass, momentum, energy and concentration equations when subject to given boundary conditions. In the context of building simulation, the Boussinesq approximation is usually applied whereby the air density is held constant and the effects of buoyancy are included within the momentum equation. In tensor notation, the conservation equations are as follows.

<u>Continuity</u>

$$\frac{\partial \rho}{\partial t} + \frac{\partial}{\partial x_i}(\rho u_i) = 0$$

<u>Momentum</u>

$$\frac{\partial(\rho u_i)}{\partial t} + \frac{\partial}{\partial x_j}(\rho u_i u_j) = -\frac{\partial \rho}{\partial x_i} + \frac{\partial}{\partial x_i}\left[\mu\left(\frac{\partial u_i}{\partial x_j} + \frac{\partial u_j}{\partial x_i}\right)\right] - \rho g \beta(\theta_\infty - \theta)$$

<u>Energy</u>

$$\frac{\partial(\rho H)}{\partial t} + \frac{\partial}{\partial x_i}(\rho u_i H) = \frac{\partial}{\partial x_i}\left[\frac{k}{C_p}\frac{\partial H}{\partial x_i}\right] + S_H$$

<u>Concentration</u>

$$\frac{\partial(\rho C)}{\partial t} + \frac{\partial}{\partial x_j}(\rho u_j C) = \frac{\partial}{\partial x_j}\left[\rho D \frac{\partial C}{\partial x_j}\right] + S_C$$

where t is time (s), x_i the co-ordinate axis (= x, y and z), ρ density (kg/m^3), u_i the velocity component in the cardinal directions (= u, v, w; m/s), p the pressure (N/m^2), g the gravitational constant (m/s^2), μ the viscosity (kg/m.s), H the specific enthalpy (J/kg.K), C the species concentration (kg/kg), k the conductivity (W/m.K), D the species diffusion coefficient (m^2/s) for moisture, CO_2 etc., C_p the specific heat (J/kg.K), β the thermal expansion coefficient of air (1/K), θ_∞ a reference temperature (°C) and S_H, S_C energy and species source terms respectively (W/m^3 and kg/m^3.s).

Direct solution of the above conservation equations is non-trivial task because extremely fine meshes are required to resolve turbulent fluctuations. Instead, the turbulence transport technique is often employed whereby the instantaneous values of temperature, concentration, velocity, pressure etc. are represented as the sum of their mean and fluctuating components, and the effect of turbulent motion is time-averaged. This gives rise to the following mean conservation equation for an incompressible fluid:

$$\frac{\partial}{\partial t}(\rho\phi) = \frac{\partial}{\partial x_i}\left(\Gamma_\phi \frac{\partial \phi}{\partial x_i} - \rho U_i \phi\right) + S_\phi$$

where φ is a transport variable such as continuity ($\varphi = 1$), enthalpy, concentration of contaminant or velocity; ρ (kg/m^3), Γ_φ a diffusion coefficient, U_i a mean velocity component (U, V, W), and S_φ a mean source term. In words, the above equation can be read as

> *The rate of increase of φ within a fluid element = the rate of increase of φ due to diffusion - the net rate of flow of φ out of the element + the rate of increase of φ due to sources.*

To overcome the difficulties of directly modelling turbulent flows, a turbulence transport model is normally used whereby the influence of turbulence on the time averaged motion of air may be determined. Of the possible turbulence transport models, the standard k-ε model is widely used because of its general applicability and reasonable accuracy. Its function is to determine the eddy viscosity at each grid point (as used in the momentum equation) as a function of local values of the turbulent kinetic energy (k) and its rate of dissipation (ε):

$$\mu_t = \rho C_\mu k^2/\varepsilon$$

where C_μ is a dimensionless constant and equations exist to estimate k and ε.

Because the standard k-ε model is valid only for turbulent flow regions, it cannot be used to represent the near-wall condition where viscous effects predominate and the flow is laminar. Instead, logarithmic wall functions are usually employed whereby the form of the velocity and temperature profile within the boundary layer is assumed in order to determine the surface shear stress and convective heat transfer. An alternative approach is to utilise wall functions derived for the specific case in hand or to replace the wall functions with empirical data.

Whatever the approach, the problem reduces to a set of time-averaged nodal conservation equations for U, V, W, H, C, k and ε. These conservation equations may be discretised by the finite volume method to obtain a set of linear equations. Because these equations are strongly coupled and highly non-linear – that is the equation coefficients and source terms are dependent on the state variables – they must be solved iteratively for a given set of boundary conditions. Moreover, when conflated with the building thermal and network air flow models, the CFD domain equations must be solved in tandem with the other domain equations and repeatedly at each time row throughout a simulation.

Initial and boundary conditions

Initial values of ρ, u_i and H are required at time t=0 for all domain cells. For solid surfaces, the required boundary conditions include the temperature (or flux) at points adjacent to the domain cells. For cells subjected to an in-flow from ventilation openings and doors/windows, the mass, momentum, energy & species exchange must be given in terms of the distribution of relevant variables of state – U, V, W, H, k, ε and C. At outlets, the normal practice is to impose a constant pressure and the conditions $\partial u_n/\partial n = 0$, $\partial H/\partial n = 0$, $\partial k/\partial n = 0$, $\partial \varepsilon /\partial n = 0$, where n indicates the direction normal to the boundary.

Iterative solution procedure

The SIMPLE (Semi-Implicit Method for Pressure-Linked Equations) method is commonly used to solve the set of elliptic flow equations. Essentially, the pressure of each domain cell is linked to the velocities connecting with surrounding cells in a manner that conserves continuity. The method accounts for the absence of an equation for pressure by establishing a modified form of the continuity equation to represent the pressure correction that would be required to ensure that the velocity components determined from the momentum equations move the solution towards continuity. This is done by using a guessed pressure field to solve the momentum equations for intermediate velocity components U, V and W. These velocities are then used to estimate the required pressure field correction from the modified continuity equation. The energy equation, and any other scalar equations (e.g. for concentration), are then solved and the process iterates until convergence is attained. To avoid numerical divergence, it is usual to apply under relaxation to the pressure correction terms.

Variants of the SIMPLE algorithm have been developed in order to reduce the computational burden and assist convergence. These include SIMPLE-Revised, in which the pressure field is obtained directly (i.e. without the need for correction) from a pressure equation derived from the continuity equation, and SIMPLE-Consistent, in which the simplifications applied to the momentum/continuity equations to obtain the pressure field correction are less onerous.

Results interpretation

The information inherent within the CFD results is usually communicated graphically. For example, figure 7 shows the distribution of the mean age of air for a representative 2D room slice, which indicates the distribution of air freshness, a prerequisite of any indoor air quality assessment. This, along with similar outputs for the other principal parameters (humidity, contaminants, radiant temperature etc.), may then be used to assess the indoor air quality and thermal discomfort according to some appropriate standard.

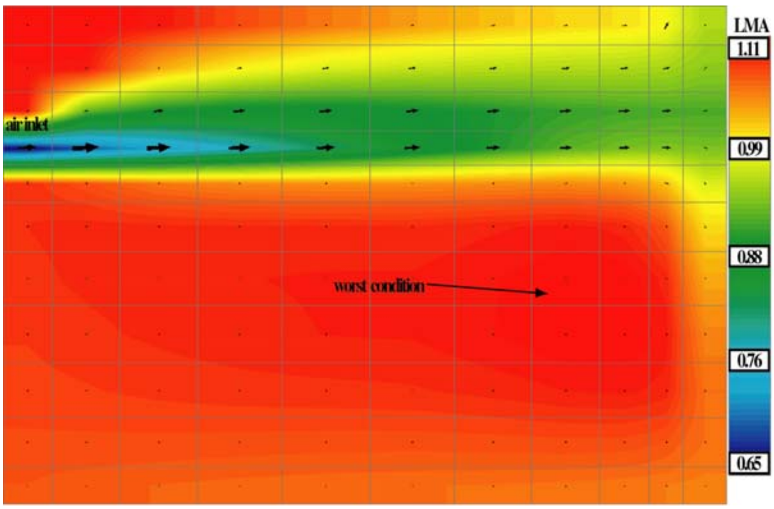

Figure 7: Distribution of the local mean age of air.

The conflation of CFD and building simulation gives rise to a significant number of relevant indicators, including but not limited to:

1. the variation in vertical air temperature between floor and head height;
2. the absolute temperature of the floor;
3. radiant temperature asymmetry;
4. unsatisfactory ventilation rate;
5. unsatisfactory CO_2 level;
6. local draught assessed on the basis of the turbulence intensity distribution;

7. additional air speed required to off-set an elevated temperature;
8. comfort check based on effective temperature;
9. mean age of air.